Article

A General Euler Angle Error Model of Strapdown Inertial Navigation Systems

Jianli Li [1,2,*] (iD)**, Pengfei Dang [2], Yiqi Li [2] and Bin Gu [2]**

[1] The National Key Lab of Satellite Navigation System and Equipment Technology, The 54th Research Institute of China Electronics Technology Group Corporation, Shijiazhuang 050002, China

[2] School of Instrument Science and Opto-Electronic Engineering, Beihang University, Beijing 100191, China; dangpengfei@buaa.edu.cn (P.D.); liyiqibuaa@163.com (Y.L.); oucgubin@163.com (B.G.)

[*] Correspondence: lijianli@buaa.edu.cn; Tel.: +86-10-8233-9550

Featured Application: The proposed general Euler angle error model can intuitively describe the process of attitude motion. Especially in large-angle attitude movements, such as missile erection and manipulator control, real-time attitude information can be measured, after which the attitude motion can be optimized.

Abstract: Attitude error models play an important role in analyzing the characteristics of navigation error propagation for the design and operation of strapdown inertial navigation systems (SINS). However, the majority of existing attitude error models focus on misalignment, rather than Euler angle errors. Misalignment cannot directly describe attitude error propagation, which is an indirect measurement. To solve the problem, a general Euler angle error model of SINS is proposed. Based on Euler angle error propagation analysis, relative Euler angle errors, and convected Euler angle errors are introduced to compose the general Euler angle error model. Simulation experiments are carried out to verify the proposed model.

Keywords: attitude error model; navigation error propagation; relative Euler angle error; convected Euler angle error

1. Introduction

Inertial navigation systems (INS) can generally be classified into gimbaled inertial navigation systems (GINS) and strapdown inertial navigation systems (SINS) [1–3]. For SINS, gyro output is used to maintain a digital computational platform as its reference frame [4,5]. Compared with GINS, SINS have many advantages, such as small size, light weight, low cost, easy maintenance, etc., gradually replacing GINS [6,7]. Whether in GINS or in SINS, attitude error models play an important role in analyzing the characteristics of navigation error propagation, implementing the Kalman filter for aided navigation systems, and detecting failures in real-time [8,9].

Attitude error formulations of GINS, including those of Psi-angle, Phi-angle, were developed for local level platform navigators [10]. With the development of SINS, Silva et al. derived attitude error formulations for stationary SINS [11]. The static model had a better application in research for its simple structure, but it did not apply to a dynamic base. Hao et al. established the dynamic error model based on the static model, where vehicle location changes would directly affect the error characteristics of SINS [12]. Assuming that the propagation characteristics of the navigation errors are linear, some linearized attitude error formulations are also modeled [13,14]. Goshen and Bar presented a SINS error model which contains all of the known models in the same framework [8]. Chen et al. proved that these linearized error models are equivalent to each other [15], but linearized error models are not effective for nonlinear systems where large navigation errors, such as in-flight alignment,

are generated [16]. Savage introduced a rotation vector error and brought in white noise for error differential equations to analyze the large attitude errors of SINS [17]. Then, quaternion and dual quaternion errors were developed to describe attitude error propagation [18,19]. As quaternions and Euler angles are not in one-to-one correspondence, both the converting relation and the corresponding relation have to be taken into consideration during an attitude control process [20]. The SINS attitude error formulations above mainly focus on misalignment for a specific computational frame rather than Euler angle errors. However, misalignment error formulations cannot describe attitude error propagation directly [21].

Euler angles are the most intuitive measurements of attitude movements, especially large-angle attitude movements. Real-time attitude information can be obtained by using Euler angles to express the attitude movement in controlled areas [22,23], then appropriate optimization can be made. An adaptive Euler-angle-based unscented Kalman filter (UKF) is utilized to analyze attitude in real-time [24]. The manipulator control process is a large-angle attitude movement process which is very sensitive to Euler angles [25,26]. The controllers for each degree of freedom are Euler angles. There are some specific applications, such as 6-DOF robot manipulators with Euler wrists [27,28], and robotic-wheelchair controllers combined with multi-sensors to obtain accurate orientation in the form of Euler angles [29]. Additionally, Jing proposed a quasi-Euler angle to control the attitude, where the terminal attitude of a satellite can be determined [20]. The control approaches mentioned above are based on Euler angles, and the Euler angle method turns out to be superior to the others in the applications because it shows better numerical accuracy, stability, and robustness [30,31].

The misalignment angle is characterized by the calculation of the three-axis deviation angle between the computational frame and the navigation frame, which cannot directly reflect and optimize a body's attitude movement. The initial attitude of the navigation system is in Euler angle form [32]. Since the output attitudes of SINS are Euler angles, it is necessary to analyze the Euler angle error model which can reflect attitude measurement accuracy more directly.

To address the above issues, a general Euler angle error modeling method of SINS is proposed. Firstly, based on the operation principles of SINS, the Euler angle solution formulation is given. Then the differential formulation of relative Euler angle errors induced by angular velocity errors can be derived. Secondly, the differential formulation of convected Euler angle errors induced by an inaccurate attitude matrix is proposed based on the Euler angle differential equations. Then, general Euler angle error formulations of SINS are modeled, and the mechanisms and characteristics of Euler angle error propagation in SINS are analyzed. Finally, some simulation experiments are carried out to verify the proposed models. The general Euler angle error model can be used to analyze the attitude movements in real-time, and an optimal control strategy can be designed based on the general Euler angle error model.

2. The Proposed General Euler Angle Error Model

The general Euler angle error model contains the relative Euler angle error model and the convected Euler angle error model. The relative Euler angle error model indicates the relationship between Euler angle errors and angular velocity errors of the body frame with respect to the navigation frame denoted in the body frame. The convected Euler angle error model indicates the relationship between Euler angle errors and Euler angles.

2.1. Attitude Solution by Euler Angle Differential Equations

Replacing the inertial platform of GINS, the digital computational platform of SINS, the computational frame inside the navigation computer, is theoretically equivalent to the local level navigation frame when there are no navigation errors. Gyro output is used to maintain the digital computational platform, and the specific force measurements from the accelerometer triads are resolved, then the velocity and position are acquired by double integration as shown in Figure 1. However, no matter which reference frame is chosen, all quantities must be transformed to the

computational frame prior to integration. How to determine the body attitude matrix is vital, because it represents the transformation of the body frame with respect to the navigation frame.
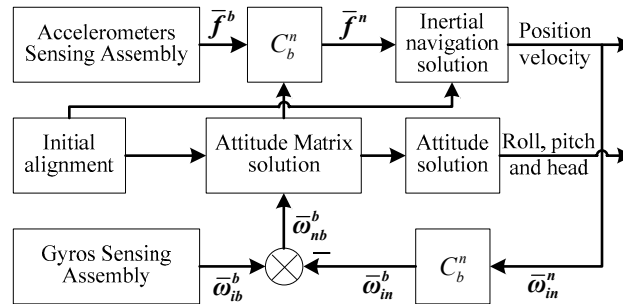

Figure 1. The operational principle of SINS (strapdown inertial navigation systems).

The body attitude matrix can be calculated by Euler angles φ, θ, and γ in turn along the head, pitch, and roll axes. These Euler angles can be resolved in real-time using the angular velocities of the body frame with respect to the navigation frame denoted in the body frame, and the angular velocity can be calculated by:

$$\omega_{nb}^b = \omega_{ib}^b - C_n^b \omega_{in}^n = \omega_{ib}^b - C_n^b(\omega_{ie}^n + \omega_{en}^n) \tag{1}$$

where ω_{ib}^b is the angular velocity vector of the body frame with respect to the inertial frame denoted in the body frame, and can be directly measured by gyros, and ω_{in}^n is the angular velocity vector of the navigation frame with respect to the inertial frame denoted in the navigation frame $\omega_{in}^n = \omega_{ie}^n + \omega_{en}^n$. ω_{ie}^n is the angular velocity vector of the Earth frame with respect to the inertial frame denoted in the navigation frame. ω_{en}^n is the angular velocity vector of the navigation frame with respect to the Earth frame denoted in the navigation frame. They can be respectively calculated by:

$$\omega_{in}^n = \omega_{ie}^n + \omega_{en}^n = \begin{bmatrix} \omega_{iex}^n \\ \omega_{iey}^n \\ \omega_{iez}^n \end{bmatrix} + \begin{bmatrix} \omega_{enx}^n \\ \omega_{eny}^n \\ \omega_{enz}^n \end{bmatrix} = \begin{bmatrix} 0 \\ \omega_{ie}\cos(L) \\ \omega_{ie}\sin(L) \end{bmatrix} + \begin{bmatrix} -V_N/(R_M + H) \\ V_E/(R_N + H) \\ V_E\tan(L)/(R_N + H) \end{bmatrix} \tag{2}$$

As shown in Figure 2, in order to accurately derive the Euler angle error differential equations, the transformation relation between the angular velocity of the body frame with respect to the navigation frame denoted in the body frame and the Euler angle velocities in head, pitch, and roll with respect to the navigation frame, can be expressed as:

$$\begin{bmatrix} \omega_{nbx}^b \\ \omega_{nby}^b \\ \omega_{nbz}^b \end{bmatrix}_b = R_y^2(\gamma)R_x^1(\theta)R_z^n(\varphi)\begin{bmatrix} 0 \\ 0 \\ \dot{\varphi}^n \end{bmatrix}_n + R_y^2(\gamma)R_x^1(\theta)\begin{bmatrix} \dot{\theta}^n \\ 0 \\ 0 \end{bmatrix}_1 + R_y^2(\gamma)\begin{bmatrix} 0 \\ \dot{\gamma}^n \\ 0 \end{bmatrix}_2 \tag{3}$$

where ω_{nbi}^b is the angular velocity of the body frame with respect to the navigation frame denoted in the body frame along i axis, $R_y^2(\gamma)$, $R_x^1(\theta)$, and $R_z^n(\varphi)$ respectively represent attitude transformation matrixes induced by Euler angles γ, θ, and φ along the roll, pitch, and head. Equation (3) can be further rewritten by Euler angles:

$$\begin{bmatrix} \omega_{nbx}^b \\ \omega_{nby}^b \\ \omega_{nbz}^b \end{bmatrix}_b = \left\{ \begin{bmatrix} \cos(\gamma) & 0 & -\sin(\gamma) \\ 0 & 1 & 0 \\ \sin(\gamma) & 0 & \cos(\gamma) \end{bmatrix} \begin{bmatrix} 1 & 0 & 0 \\ 0 & \cos(\theta) & \sin(\theta) \\ 0 & -\sin(\theta) & \cos(\theta) \end{bmatrix} \begin{bmatrix} 0 \\ 0 \\ \dot{\varphi} \end{bmatrix}_n + \begin{bmatrix} \cos(\gamma) & 0 & -\sin(\gamma) \\ 0 & 1 & 0 \\ \sin(\gamma) & 0 & \cos(\gamma) \end{bmatrix} \begin{bmatrix} \dot{\theta} \\ 0 \\ 0 \end{bmatrix}_1 + \begin{bmatrix} 0 \\ \dot{\gamma} \\ 0 \end{bmatrix}_2 \right\}$$
$$= \begin{bmatrix} -\sin(\gamma)\cos(\theta) & \cos(\gamma) & 0 \\ \sin(\theta) & 0 & 1 \\ \cos(\gamma)\cos(\theta) & \sin(\gamma) & 0 \end{bmatrix} \begin{bmatrix} \dot{\varphi} \\ \dot{\theta} \\ \dot{\gamma} \end{bmatrix} \tag{4}$$
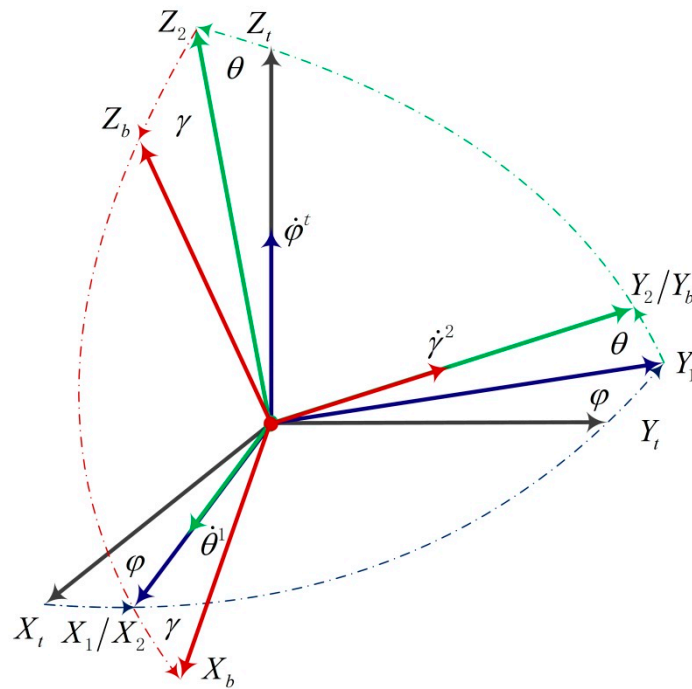
Figure 2. The Euler angles transformation relation for SINS.

From Equation (4), the Euler angle velocities induced by the angular velocities of the body frame with respect to the navigation frame denoted in the body frame can be written as:

$$
\begin{bmatrix} \dot{\varphi} \\ \dot{\theta} \\ \dot{\gamma} \end{bmatrix} = \begin{bmatrix} -\sin(\gamma)\cos(\theta) & \cos(\gamma) & 0 \\ \sin(\theta) & 0 & 1 \\ \cos(\gamma)\cos(\theta) & \sin(\gamma) & 0 \end{bmatrix}^{-1} \begin{bmatrix} \omega_{nbx}^b \\ \omega_{nby}^b \\ \omega_{nbz}^b \end{bmatrix}_b
$$
$$
= \frac{1}{\cos(\theta)} \begin{bmatrix} -\sin(\gamma) & 0 & \cos(\gamma) \\ \cos(\theta)\cos(\gamma) & 0 & \cos(\theta)\sin(\gamma) \\ \sin(\theta)\sin(\gamma) & \cos(\theta) & -\sin(\theta)\cos(\gamma) \end{bmatrix} \begin{bmatrix} \omega_{nbx}^b \\ \omega_{nby}^b \\ \omega_{nbz}^b \end{bmatrix}_b \qquad (5)
$$
$$
= \begin{bmatrix} -\frac{\sin(\gamma)}{\cos(\theta)}\omega_{nbx}^b + \frac{\cos(\gamma)}{\cos(\theta)}\omega_{nbz}^b \\ \cos(\gamma)\omega_{nbx}^b + \sin(\gamma)\omega_{nbz}^b \\ \tan(\theta)\sin(\gamma)\omega_{nbx}^b + \omega_{nby}^b - \tan(\theta)\cos(\gamma)\omega_{nbz}^b \end{bmatrix}
$$

According to Equation (5), the Euler angles can be calculated by introducing the integral operation:

$$
\varphi = \varphi_0 + \int_{t0}^{t} \dot{\varphi}\,dt = \varphi_0 + \int_{t0}^{t} \left[-\frac{\sin(\gamma)}{\cos(\theta)}\omega_{nbx}^b + \frac{\cos(\gamma)}{\cos(\theta)}\omega_{nbz}^b \right] dt \qquad (6)
$$

$$
\theta = \theta_0 + \int_{t0}^{t} \dot{\theta}\,dt = \theta_0 + \int_{t0}^{t} \left[\cos(\gamma)\omega_{nbx}^b + \sin(\gamma)\omega_{nbz}^b \right] dt \qquad (7)
$$

$$
\gamma = \gamma_0 + \int_{t0}^{t} \dot{\gamma}\,dt = \gamma_0 + \int_{t0}^{t} \left[\tan(\theta)\sin(\gamma)\omega_{nbx}^b + \omega_{nby}^b - \tan(\theta)\cos(\gamma)\omega_{nbz}^b \right] dt \qquad (8)
$$

where φ_0, θ_0, and γ_0 respectively represent the initial head, pitch, and roll of the SINS. According to Equations (6)–(8), the body attitude matrix from the navigation frame to the body frame can be expressed by Euler angles φ, θ, and γ in the head, pitch, and roll:

$$
\begin{aligned}
C_n^b &= \begin{bmatrix} \cos(\gamma)\cos(\varphi) - \sin(\gamma)\sin(\varphi)\sin(\theta) & \cos(\gamma)\sin(\varphi) + \sin(\gamma)\cos(\varphi)\sin(\theta) & -\sin(\gamma)\cos(\theta) \\ -\sin(\varphi)\cos(\theta) & \cos(\varphi)\cos(\theta) & \sin(\theta) \\ \sin(\gamma)\cos(\varphi) + \cos(\gamma)\sin(\varphi)\sin(\theta) & \sin(\gamma)\sin(\varphi) - \cos(\gamma)\cos(\varphi)\sin(\theta) & \cos(\gamma)\cos(\theta) \end{bmatrix} \\
&= \begin{bmatrix} T_{11} & T_{12} & T_{13} \\ T_{21} & T_{22} & T_{23} \\ T_{31} & T_{32} & T_{33} \end{bmatrix}
\end{aligned}
\tag{9}
$$

where T_{ij} is the element of the transformation matrix C_n^b with $i = 1, 2, 3$; $j = 1, 2, 3$.

2.2. Modeling of Relative Euler Angle Errors

The coordinate systems and transformation relation for SINS are shown in Figure 3. The misalignment are computational platform angle errors with respect to the navigation frame in the navigation system [33]. Generally, it is a small angle from the navigation frame $o_n x_n y_n z_n$ to the SINS computational frame $o_c x_c y_c z_c$, and can be expressed by a variable $\boldsymbol{\Phi} = \begin{bmatrix} \phi_E & \phi_N & \phi_V \end{bmatrix}^T$ with ϕ_i being misalignment along the east, north, and vertical directions. The coordinate transformation matrix from the navigation frame $o_n x_n y_n z_n$ to the computational frame $o_c x_c y_c z_c$ is referred to as an attitude matrix, and can be written as:

$$
\begin{aligned}
C_n^c &= \begin{bmatrix} \cos(\phi_N) & 0 & -\sin(\phi_N) \\ 0 & 1 & 0 \\ \sin(\phi_N) & 0 & \cos(\phi_N) \end{bmatrix} \begin{bmatrix} 1 & 0 & 0 \\ 0 & \cos(\phi_E) & \sin(\phi_E) \\ 0 & -\sin(\phi_E) & \cos(\phi_E) \end{bmatrix} \begin{bmatrix} \cos(\phi_V) & \sin(\phi_V) & 0 \\ -\sin(\phi_V) & \cos(\phi_V) & 0 \\ 0 & 0 & 1 \end{bmatrix} \\
&\approx I - \begin{bmatrix} (\phi_N^2 + \phi_V^2)/2 & -(\phi_V + \phi_E\phi_N) & \phi_N \\ \phi_N & (\phi_E^2 + \phi_V^2)/2 & -\phi_E \\ -(\phi_N + \phi_E\phi_V) & (\phi_E + \phi_N\phi_V) & (\phi_E^2 + \phi_N^2)/2 \end{bmatrix} \\
&\approx I - \begin{bmatrix} 0 & -\phi_V & \phi_N \\ \phi_V & 0 & -\phi_E \\ -\phi_N & \phi_E & 0 \end{bmatrix} = I - (\boldsymbol{\Phi} \times)
\end{aligned}
\tag{10}
$$

where ϕ_E, ϕ_N, ϕ_V are small angles, and $\cos(\phi_E) = \cos(\phi_N) = \cos(\phi_V) \approx 1$, $\sin(\phi_E) \approx \phi_E$, $\sin(\phi_N) \approx \phi_N$, $\sin(\phi_V) \approx \phi_V$. According to Equations (9) and (10), the body attitude matrix from the computational frame to the body frame can be calculated as:

$$
\begin{aligned}
C_c^b &= C_n^b C_c^n = \begin{bmatrix} T_{11} & T_{12} & T_{13} \\ T_{21} & T_{22} & T_{23} \\ T_{31} & T_{32} & T_{33} \end{bmatrix} \begin{bmatrix} 1 & -\phi_V & \phi_N \\ \phi_V & 1 & -\phi_E \\ -\phi_N & \phi_E & 1 \end{bmatrix} \\
&= \begin{bmatrix} \cos(\gamma^c)\cos(\varphi^c) - \sin(\gamma^c)\sin(\varphi^c)\sin(\theta^c) & \cos(\gamma^c)\sin(\varphi^c) + \sin(\gamma^c)\cos(\varphi^c)\sin(\theta^c) & -\sin(\gamma^c)\cos(\theta^c) \\ -\sin(\varphi^c)\cos(\theta^c) & \cos(\varphi^c)\cos(\theta^c) & \sin(\theta^c) \\ \sin(\gamma^c)\sin(\varphi^c) + \cos(\gamma^c)\sin(\varphi^c)\sin(\theta^c) & \sin(\gamma^c)\sin(\varphi^c) - \cos(\gamma^c)\cos(\varphi^c)\sin(\theta^c) & \cos(\gamma^c)\cos(\theta^c) \end{bmatrix} \\
&= \begin{bmatrix} C_{11} & C_{12} & C_{13} \\ C_{21} & C_{22} & C_{23} \\ C_{31} & C_{32} & C_{33} \end{bmatrix}
\end{aligned}
\tag{11}
$$

where φ^c, θ^c, and γ^c are the head, pitch, and roll with respect to the computational frame $o_c x_c y_c z_c$, and C_{ij} is an element of the transformation matrix C_c^b with $i = 1, 2, 3$; $j = 1, 2, 3$.
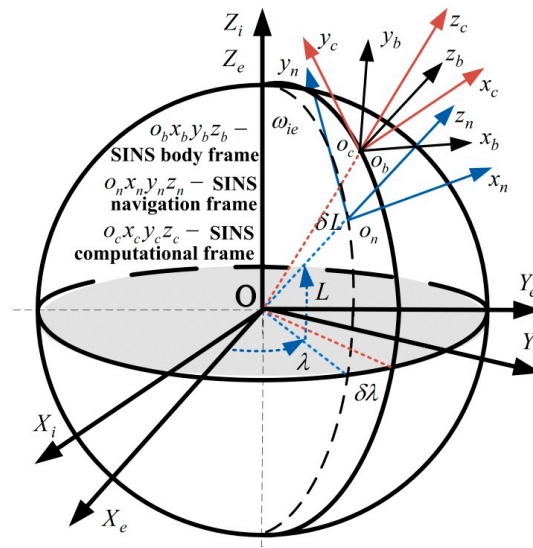
Figure 3. The coordinate systems and transformation relation for SINS.

Since the misalignment $\boldsymbol{\Phi}$ from the navigation frame $o_n x_n y_n z_n$ to the computational frame $o_c x_c y_c z_c$, according to Equation (11), the transformation relation among attitude matrixes can be expressed as:

$$C_b^c = C_n^c C_b^n = [I - (\boldsymbol{\Phi} \times)] C_b^n \tag{12}$$

$$\delta C_b^n = C_b^c - C_b^n = -(\boldsymbol{\Phi} \times) C_b^n \tag{13}$$

$$\dot{\delta C}_b^n = -\left(\dot{\boldsymbol{\Phi}} \times \right) C_b^n - (\boldsymbol{\Phi} \times) C_b^n \boldsymbol{\omega}_{nb}^b \times \tag{14}$$

where δC_b^n represents the error of attitude transformation matrix from the body frame $o_b x_b y_b z_b$ to the navigation frame $o_n x_n y_n z_n$. The differential equation of attitude transformation matrix for SINS can be given by:

$$\dot{C}_b^n = C_b^n (\boldsymbol{\omega}_{nb}^b \times) = C_b^n \left[\left(\boldsymbol{\omega}_{ib}^b - C_n^b \boldsymbol{\omega}_{in}^n \right) \times \right] = C_b^n \left[\left(\boldsymbol{\omega}_{ib}^b - C_n^b (\boldsymbol{\omega}_{ie}^n + \boldsymbol{\omega}_{en}^n) \right) \times \right] \tag{15}$$

The SINS output includes not only sensing the angular velocity $\boldsymbol{\omega}_{ib}^b$, but also harmful measurement error $\delta \boldsymbol{\omega}_{ib}^b$ and random drift of gyros ε^b, and can be expressed as:

$$\hat{\boldsymbol{\omega}}_{ib}^b = \boldsymbol{\omega}_{ib}^b + \delta \boldsymbol{\omega}_{ib}^b + \varepsilon^b \tag{16}$$

The computational angular velocity of the computational frame with respect to the inertial frame denoted in the computational frame has errors, and can be expressed as:

$$\boldsymbol{\omega}_{ic}^c = \boldsymbol{\omega}_{in}^n + \delta \boldsymbol{\omega}_{in}^n = \boldsymbol{\omega}_{ie}^n + \boldsymbol{\omega}_{en}^n + \delta \boldsymbol{\omega}_{ie}^n + \delta \boldsymbol{\omega}_{en}^n \tag{17}$$

where $\delta \boldsymbol{\omega}_{in}^n$ is the angular velocity error of the navigation frame with respect to the inertial frame denoted in the navigation frame $\delta \boldsymbol{\omega}_{in}^n = \delta \boldsymbol{\omega}_{ie}^n + \delta \boldsymbol{\omega}_{en}^n$, and $\delta \boldsymbol{\omega}_{ie}^n$ is the angular velocity error of the Earth frame with respect to the inertial frame denoted in the navigation frame. $\delta \boldsymbol{\omega}_{en}^n$ is the angular velocity error of the navigation frame with respect to the earth frame denoted in the navigation frame.

According to Equation (15), the differential equation of attitude transformation matrix from the body frame $o_b x_b y_b z_b$ to the computational frame $o_c x_c y_c z_c$ can be given by:

$$\dot{C}_b^c = C_b^c \left[\left(\hat{\boldsymbol{\omega}}_{ib}^b - C_c^b \boldsymbol{\omega}_{ic}^c \right) \times \right] \tag{18}$$

According to Equation (13), the differential equation of attitude transformation matrix $\dot{C}_b^c$ can also be given by:

$$\dot{C}_b^c = \dot{C}_b^n + \delta\dot{C}_b^n \tag{19}$$

Substituting Equations (16), (17) and (19) into Equation (18), the differential equation of the attitude transformation matrix can be rewritten as:

$$\dot{C}_b^n + \delta\dot{C}_b^n = [I - (\boldsymbol{\Phi}\times)]C_b^n\left\{\left[\boldsymbol{\omega}_{ib}^b + \delta\boldsymbol{\omega}_{ib}^b + \boldsymbol{\varepsilon}^b - C_n^b(I + \boldsymbol{\Phi}\times)(\boldsymbol{\omega}_{in}^n + \delta\boldsymbol{\omega}_{in}^n)\right]\times\right\} \tag{20}$$

Substituting Equation (15) into Equation (20), supposing that the attitude error is slight and ignoring the term as small as the second order and the high-order terms of error products, it is easy to obtain the differential equation of attitude transformation matrix errors:

$$\delta\dot{C}_b^n = C_b^n\left(\delta\boldsymbol{\omega}_{ib}^b\times\right) + C_b^n\left(\boldsymbol{\varepsilon}^b\times\right) - C_b^n\left[\left(\boldsymbol{\Phi}\times\boldsymbol{\omega}_{in}^b\right)\times\right] - C_b^n\left(\delta\boldsymbol{\omega}_{in}^b\times\right) - (\boldsymbol{\Phi}\times)C_b^n\left(\boldsymbol{\omega}_{nb}^b\times\right) \tag{21}$$

Substituting Equation (14) into Equation (21), the differential equation of attitude transformation matrix errors can be rewritten as:

$$-\left(\dot{\boldsymbol{\Phi}}\times\right)C_b^n - (\boldsymbol{\Phi}\times)C_b^n(\boldsymbol{\omega}_{nb}^b\times) = C_b^n(\delta\boldsymbol{\omega}_{ib}^b\times) + C_b^n(\boldsymbol{\varepsilon}^b\times) - C_b^n\left[(\boldsymbol{\Phi}\times\boldsymbol{\omega}_{in}^b)\times\right] - C_b^n(\delta\boldsymbol{\omega}_{in}^b\times) - (\boldsymbol{\Phi}\times)C_b^n(\boldsymbol{\omega}_{nb}^b\times) \tag{22}$$

The differential equation of misalignment of SINS can be further rewritten as:

$$\left(\dot{\boldsymbol{\Phi}}\times\right) = -[(\boldsymbol{\omega}_{in}^n\times\boldsymbol{\Phi})\times] + (\delta\boldsymbol{\omega}_{in}^n\times) - \left[\left(C_b^n\delta\boldsymbol{\omega}_{ib}^b\right)\times\right] - \left[\left(C_b^n\boldsymbol{\varepsilon}^b\right)\times\right] \tag{23}$$

$$\dot{\boldsymbol{\Phi}} = -\boldsymbol{\omega}_{in}^n\times\boldsymbol{\Phi} + \delta\boldsymbol{\omega}_{in}^n - C_b^n\delta\boldsymbol{\omega}_{ib}^b - C_b^n\boldsymbol{\varepsilon}^b \tag{24}$$

The differential equation of misalignment errors can be expanded as:

$$\begin{bmatrix}\dot{\phi}_E\\\dot{\phi}_N\\\dot{\phi}_V\end{bmatrix} = \begin{bmatrix}0 & -\left(\omega_{ie}\sin(L) + \frac{V_E\tan(L)}{(R_N+H)}\right) & \left(\omega_{ie}\cos(L) + \frac{V_E}{(R_N+H)}\right)\\ \left(\omega_{ie}\sin(L) + \frac{V_E\tan(L)}{R_N+H}\right) & 0 & -\frac{V_N}{(R_M+H)}\\ -\left(\omega_{ie}\cos(L) + \frac{V_E}{(R_N+H)}\right) & \frac{V_N}{(R_M+H)} & 0\end{bmatrix}\begin{bmatrix}\phi_E\\\phi_N\\\phi_V\end{bmatrix}$$
$$+ \begin{bmatrix}-\frac{\delta V_N}{(R_M+H)} + \frac{V_N}{(R_M+H)^2}\delta H + \delta\omega_{ibE}^n + \varepsilon_E\\ \frac{\delta V_E}{(R_N+H)} - \omega_{ie}\sin(L)\delta L - \frac{V_E}{(R_N+H)^2}\delta H + \delta\omega_{ibN}^n + \varepsilon_N\\ \frac{\tan(L)\delta V_E}{(R_N+H)} + \left(\omega_{ie}\cos(L) + \frac{V_E\sec^2(L)}{(R_N+H)}\right)\delta L - \frac{\tan(L)V_E}{(R_N+H)^2}\delta H + \delta\omega_{ibV}^n + \varepsilon_V\end{bmatrix} \tag{25}$$

According to Equations (16) and (17), the angular velocity error vector of the body frame $o_bx_by_bz_b$ with respect to the navigation frame $o_nx_ny_nz_n$ denoted in the body frame $o_bx_by_bz_b$ is a main factor leading to the Euler angle error, and can be expressed by:

$$\delta\boldsymbol{\omega}_{nb}^b = \delta\boldsymbol{\omega}_{ib}^b + \boldsymbol{\varepsilon}^b - \delta\boldsymbol{\omega}_{in}^b = \begin{bmatrix}\delta\omega_{ibx}^b + \varepsilon_x^b - \delta\omega_{inx}^b\\ \delta\omega_{iby}^b + \varepsilon_y^b - \delta\omega_{iny}^b\\ \delta\omega_{ibz}^b + \varepsilon_z^b - \delta\omega_{inz}^b\end{bmatrix} \tag{26}$$

The angular velocity error vector of the navigation frame with respect to the inertial frame denoted in the body frame can be rewritten as:

$$\delta\boldsymbol{\omega}_{in}^b = \boldsymbol{\omega}_{ic}^b - \boldsymbol{\omega}_{in}^b = C_c^b\boldsymbol{\omega}_{ic}^c - C_n^b\boldsymbol{\omega}_{in}^n = C_c^b(\boldsymbol{\omega}_{in}^n + \delta\boldsymbol{\omega}_{in}^n) - C_c^b(I - \Phi\times)\boldsymbol{\omega}_{in}^n = C_c^b\delta\boldsymbol{\omega}_{in}^n + C_c^b\Phi\times\boldsymbol{\omega}_{in}^n \tag{27}$$

where ω_{in}^{n} is the angular velocity vector of the navigation frame with respect to the inertial frame denoted in the navigation frame, and can be found in Equation (2). $\delta\omega_{in}^{n}$ is an angular velocity error vector of the navigation frame with respect to the inertial frame denoted in the navigation frame, as shown in Equation (17). According to Equation (27), the angular velocity error of the navigation frame with respect to the inertial frame denoted in the body frame is rewritten as:

$$
\begin{aligned}
\begin{bmatrix} \delta\omega_{inx}^{b} \\ \delta\omega_{iny}^{b} \\ \delta\omega_{inz}^{b} \end{bmatrix}
&= \begin{bmatrix} c_{11} & c_{12} & c_{13} \\ c_{21} & c_{22} & c_{23} \\ c_{31} & c_{32} & c_{33} \end{bmatrix} \left\{ \begin{bmatrix} 0 & -\phi_V & \phi_N \\ \phi_V & 0 & -\phi_E \\ -\phi_N & \phi_E & 0 \end{bmatrix} \begin{bmatrix} \omega_{inx}^{n} \\ \omega_{iny}^{n} \\ \omega_{inz}^{n} \end{bmatrix} + \begin{bmatrix} \delta\omega_{inx}^{n} \\ \delta\omega_{iny}^{n} \\ \delta\omega_{inz}^{n} \end{bmatrix} \right\} \\
&= \begin{bmatrix} c_{11} & c_{12} & c_{13} \\ c_{21} & c_{22} & c_{23} \\ c_{31} & c_{32} & c_{33} \end{bmatrix} \left\{ \begin{bmatrix} 0 & -\phi_V & \phi_N \\ \phi_V & 0 & -\phi_E \\ -\phi_N & \phi_E & 0 \end{bmatrix} \begin{bmatrix} -\frac{V_N}{(R_M+H)} \\ \omega_{ie}\cos(L)+\frac{V_E}{(R_N+H)} \\ \omega_{ie}\sin(L)+\frac{V_E\tan(L)}{(R_N+H)} \end{bmatrix} + \begin{bmatrix} -\frac{\delta V_N}{(R_M+H)}+\frac{V_N}{(R_M+H)^2}\delta H \\ \frac{\delta V_E}{(R_N+H)}-\omega_{ie}\sin(L)\delta L-\frac{V_E}{(R_N+H)^2}\delta H \\ \frac{\tan(L)\delta V_E}{(R_N+H)}+\left(\omega_{ie}\cos(L)+\frac{V_E\sec^2(L)}{(R_N+H)}\right)\delta L-\frac{\tan(L)V_E}{(R_N+H)^2}\delta H \end{bmatrix} \right\}
\end{aligned}
\tag{28}
$$

where $\delta\omega_{inx}^{b}$, $\delta\omega_{iny}^{b}$, $\delta\omega_{inz}^{b}$ are angular velocity errors of the navigation frame with respect to the inertial frame denoted in the body frame.

According to Equations (5) and (28), the differential equation of the relative Euler angle error caused by angular velocity errors of the body frame with respect to the navigation frame denoted in the body frame, can be written as:

$$
\begin{aligned}
\begin{bmatrix} \dot{\delta\theta}^{\otimes} \\ \dot{\delta\gamma}^{\otimes} \\ \dot{\delta\varphi}^{\otimes} \end{bmatrix}
&\approx \frac{1}{\cos(\theta^c)} \begin{bmatrix} \cos(\theta^c)\cos(\gamma^c) & 0 & \cos(\theta^c)\sin(\gamma^c) \\ \sin(\theta^c)\sin(\gamma^c) & \cos(\theta^c) & -\sin(\theta^c)\cos(\gamma^c) \\ -\sin(\gamma^c) & 0 & \cos(\gamma^c) \end{bmatrix} \begin{bmatrix} \delta\omega_{nbx}^{b} \\ \delta\omega_{nby}^{b} \\ \delta\omega_{nbz}^{b} \end{bmatrix} \\
&= \frac{1}{\cos(\theta^c)} \begin{bmatrix} \cos(\theta^c)\cos(\gamma^c) & 0 & \cos(\theta^c)\sin(\gamma^c) \\ \sin(\theta^c)\sin(\gamma^c) & \cos(\theta^c) & -\sin(\theta^c)\cos(\gamma^c) \\ -\sin(\gamma^c) & 0 & \cos(\gamma^c) \end{bmatrix} \begin{bmatrix} \delta\omega_{ibx}^{b}+\varepsilon_x^{b}-\delta\omega_{inx}^{b} \\ \delta\omega_{iby}^{b}+\varepsilon_y^{b}-\delta\omega_{iny}^{b} \\ \delta\omega_{ibz}^{b}+\varepsilon_z^{b}-\delta\omega_{inz}^{b} \end{bmatrix} \\
&= \frac{1}{\cos(\theta^c)} \begin{bmatrix} \cos(\theta^c)\cos(\gamma^c) & 0 & \cos(\theta^c)\sin(\gamma^c) \\ \sin(\theta^c)\sin(\gamma^c) & \cos(\theta^c) & -\sin(\theta^c)\cos(\gamma^c) \\ -\sin(\gamma^c) & 0 & \cos(\gamma^c) \end{bmatrix} \\
&\quad \left\{ \begin{bmatrix} \delta\omega_{ibx}^{b}+\varepsilon_x^{b} \\ \delta\omega_{iby}^{b}+\varepsilon_y^{b} \\ \delta\omega_{ibz}^{b}+\varepsilon_z^{b} \end{bmatrix} - \begin{bmatrix} c_{11} & c_{12} & c_{13} \\ c_{21} & c_{22} & c_{23} \\ c_{31} & c_{32} & c_{33} \end{bmatrix} \left\{ \begin{bmatrix} 0 & -\phi_V & \phi_N \\ \phi_V & 0 & -\phi_E \\ -\phi_N & \phi_E & 0 \end{bmatrix} \begin{bmatrix} -\frac{V_N}{(R_M+H)} \\ \omega_{ie}\cos(L)+\frac{V_E}{(R_N+H)} \\ \omega_{ie}\sin(L)+\frac{V_E\tan(L)}{(R_N+H)} \end{bmatrix} + \begin{bmatrix} -\frac{\delta V_N}{(R_M+H)}+\frac{V_N\delta H}{(R_M+H)^2} \\ \frac{\delta V_E}{(R_N+H)}-\omega_{ie}\sin(L)\delta L-\frac{V_E\delta H}{(R_N+H)^2} \\ \frac{\tan(L)\delta V_E}{(R_N+H)}+\left(\omega_{ie}\cos(L)+\frac{V_E\sec^2(L)}{(R_N+H)}\right)\delta L-\frac{\tan(L)V_E\delta H}{(R_N+H)^2} \end{bmatrix} \right\} \right\}
\end{aligned}
\tag{29}
$$

According to Equation (29), the relative Euler angle error can be written as:

$$
\begin{bmatrix} \delta\theta^{\otimes} \\ \delta\gamma^{\otimes} \\ \delta\varphi^{\otimes} \end{bmatrix} = \begin{bmatrix} \delta\theta_0 + \int_{t0}^{t} \dot{\delta\theta}^{\otimes} dt \\ \delta\gamma_0 + \int_{t0}^{t} \dot{\delta\gamma}^{\otimes} dt \\ \delta\varphi_0 + \int_{t0}^{t} \dot{\delta\varphi}^{\otimes} dt \end{bmatrix}
\tag{30}
$$

where $\delta\theta^{\otimes}$, $\delta\gamma^{\otimes}$, $\delta\varphi^{\otimes}$ are Euler angle errors caused by $\delta\omega_{nbx}^{b}$, $\delta\omega_{nby}^{b}$, $\delta\omega_{nbz}^{b}$, and these Euler angle errors are called the relative Euler angle errors.

2.3. Modeling of Convected Euler Angle Errors

For SINS, there are Euler angle errors between head φ^c, pitch θ^c, and roll γ^c with respect to the computational frame $o_c x_c y_c z_c$ and head φ, pitch θ, and roll γ with respect to the navigation frame $o_n x_n y_n z_n$. These Euler angle errors are different from misalignment, and can be expressed as:

$$
\begin{bmatrix} \delta\varphi \\ \delta\theta \\ \delta\gamma \end{bmatrix} = \begin{bmatrix} \varphi^c \\ \theta^c \\ \gamma^c \end{bmatrix} - \begin{bmatrix} \varphi \\ \theta \\ \gamma \end{bmatrix}
\tag{31}
$$

According to Equations (5) and (31), the differential equations of Euler angle errors in head, pitch, and roll can be obtained. The differential equation of the pitch angle error is written by:

$$\begin{aligned} \delta\dot{\theta} &= \dot{\theta}^c - \dot{\theta} = \cos(\gamma^c)\omega_{nbx}^b + \sin(\gamma^c)\omega_{nbz}^b - \left[\cos(\gamma^c - \delta\gamma)\omega_{nbx}^b + \sin(\gamma^c - \delta\gamma)\omega_{nbz}^b\right] \\ &= [1 - \cos(\delta\gamma)]\left[\cos(\gamma^c)\omega_{nbx}^b + \sin(\gamma^c)\omega_{nbz}^b\right] + \left[\cos(\gamma^c)\omega_{nbz}^b - \sin(\gamma^c)\omega_{nbx}^b\right]\sin(\delta\gamma) \end{aligned} \tag{32}$$

By Taylor expansion, $\sin(\delta\gamma) \approx \delta\gamma$, $\cos(\delta\gamma) \approx 1 - (\delta\gamma)^2/2$, and the differential equation of pitch angle error can be rewritten as:

$$\delta\dot{\theta} = \left[\cos(\gamma^c)\omega_{nbz}^b - \sin(\gamma^c)\omega_{nbx}^b\right]\delta\gamma + (\delta\gamma)^2\left[\cos(\gamma^c)\omega_{nbx}^b + \sin(\gamma^c)\omega_{nbz}^b\right]/2 \tag{33}$$

Ignoring the term as small as the second order, the differential equation of pitch angle errors can be written as:

$$\delta\dot{\theta} \approx \left[\cos(\gamma^c)\omega_{nbz}^b - \sin(\gamma^c)\omega_{nbx}^b\right]\delta\gamma \tag{34}$$

Similarly, the differential equation of the roll angle error can be obtained as:

$$\delta\dot{\gamma} = \dot{\gamma}^c - \dot{\gamma} = \tan(\theta^c)\left[\sin(\gamma^c)\omega_{nbx}^b - \cos(\gamma^c)\omega_{nbz}^b\right] + \omega_{nby}^b - \tan(\theta^c - \delta\theta)\left[\sin(\gamma^c - \delta\gamma)\omega_{nbx}^b - \cos(\gamma^c - \delta\gamma)\omega_{nbz}^b\right] - \omega_{nby}^b \tag{35}$$

Based on Taylor expansion, $\tan(\theta^c - \delta\theta) = \tan(\theta^c) - \sec^2(\theta^c)\delta\theta$, $\sin(\delta\theta) \approx \delta\theta$, and the differential equation of roll angle error can be rewritten as:

$$\begin{aligned} \delta\dot{\gamma} = \ &\tan(\theta^c)\left\{\left[\cos(\gamma^c)\omega_{nbx}^b + \sin(\gamma^c)\omega_{nbz}^b\right]\delta\gamma + \left[\sin(\gamma^c)\omega_{nbx}^b - \cos(\gamma^c)\omega_{nbz}^b\right](\delta\gamma)^2/2\right\} + \\ &\sec^2(\theta^c)\delta\theta\left\{\left[\sin(\gamma^c)\omega_{nbx}^b - \cos(\gamma^c)\omega_{nbz}^b\right] - \left[\cos(\gamma^c)\omega_{nbx}^b + \sin(\gamma^c)\omega_{nbz}^b\right]\delta\gamma - \left[\sin(\gamma^c)\omega_{nbx}^b - \cos(\gamma^c)\omega_{nbz}^b\right](\delta\gamma)^2/2\right\} \end{aligned} \tag{36}$$

Ignoring the term as small as second order, the differential equation of the roll angle error can be rewritten as:

$$\delta\dot{\gamma} = \tan(\theta^c)\left[\cos(\gamma^c)\omega_{nbx}^b + \sin(\gamma^c)\omega_{nbz}^b\right]\delta\gamma + \sec^2(\theta^c)\left[\sin(\gamma^c)\omega_{nbx}^b - \cos(\gamma^c)\omega_{nbz}^b\right]\delta\theta \tag{37}$$

Assuming $\cos(\delta\theta) \approx 1 - (\delta\theta)^2/2$, $\cos(\delta\gamma) \approx 1 - (\delta\gamma)^2/2$, $\sin(\delta\theta) \approx \delta\theta$, $\sin(\delta\gamma) \approx \delta\gamma$, and the differential equation of the head angle error can be written as:

$$\begin{aligned} \delta\dot{\varphi} &= \dot{\varphi}^c - \dot{\varphi} = -\frac{1}{\cos(\theta^c)}\left[\sin(\gamma^c)\omega_{nbx}^b - \cos(\gamma^c)\omega_{nbz}^b\right] + \frac{1}{\cos(\theta^c - \delta\theta)}\left[\sin(\gamma^c - \delta\gamma)\omega_{nbx}^b - \cos(\gamma^c - \delta\gamma)\omega_{nbz}^b\right] \\ &\approx \frac{1}{\cos(\theta^c)[\cos(\delta\theta) + \tan(\theta^c)\delta\theta]}\left\{\begin{array}{l}\left[\cos(\gamma^c)\omega_{nbz}^b - \sin(\gamma^c)\omega_{nbx}^b\right][\cos(\delta\theta) + \tan(\theta^c)\delta\theta] + \\ \left[\sin(\gamma^c) - \sin(\gamma^c)(\delta\gamma)^2/2 - \cos(\gamma^c)\delta\gamma\right]\omega_{nbx}^b - \\ \left[\cos(\gamma^c) - \cos(\gamma^c)(\delta\gamma)^2/2 + \sin(\gamma^c)\delta\gamma\right]\omega_{nbz}^b\end{array}\right\} \\ &= \frac{1}{\cos(\theta^c)[\cos(\delta\theta) + \tan(\theta^c)\delta\theta]}\left\{\begin{array}{l}\left[\cos(\gamma^c)\omega_{nbz}^b - \sin(\gamma^c)\omega_{nbx}^b\right]\tan(\theta^c)\delta\theta - \\ \left[\cos(\gamma^c)\omega_{nbz}^b - \sin(\gamma^c)\omega_{nbx}^b\right](\delta\theta)^2/2 - \\ \left[\cos(\gamma^c)\omega_{nbx}^b + \sin(\gamma^c)\omega_{nbz}^b\right]\delta\gamma + \\ \left[\cos(\gamma^c)\omega_{nbz}^b - \sin(\gamma^c)\omega_{nbx}^b\right](\delta\gamma)^2/2\end{array}\right\} \end{aligned} \tag{38}$$

Based on Taylor expansion, $\sec(\theta^c - \delta\theta) \approx \sec(\theta^c) - \sec(\theta^c)\tan(\theta^c)\delta\theta$, and the differential equation of the head angle error can be rewritten as:

$$\delta\dot{\varphi} = [\sec(\theta^c) - \sec(\theta^c)\tan(\theta^c)\delta\theta]\left\{\begin{array}{l}\left[\cos(\gamma^c)\omega_{nbz}^b - \sin(\gamma^c)\omega_{nbx}^b\right]\tan(\theta^c)\delta\theta - \left[\cos(\gamma^c)\omega_{nbz}^b - \sin(\gamma^c)\omega_{nbx}^b\right](\delta\theta)^2/2 - \\ \left[\cos(\gamma^c)\omega_{nbx}^b + \sin(\gamma^c)\omega_{nbz}^b\right]\delta\gamma - \left[\cos(\gamma^c)\omega_{nbz}^b - \sin(\gamma^c)\omega_{nbx}^b\right](\delta\gamma)^2/2\end{array}\right\} \tag{39}$$

When ignoring the term as small as second order, the differential equation of head angle error can be rewritten as:

$$\delta\dot\varphi \approx \sec(\theta^c)\left\{\left[\cos(\gamma^c)\omega_{nbz}^b - \sin(\gamma^c)\omega_{nbx}^b\right]\tan(\theta^c)\delta\theta - \left[\cos(\gamma^c)\omega_{nbx}^b + \sin(\gamma^c)\omega_{nbz}^b\right]\delta\gamma\right\} \quad (40)$$

According to Equations (34), (37) and (40), the differential equation of the convected Euler angle errors can be obtained as:

$$\begin{bmatrix}\delta\dot\theta^* \\ \delta\dot\gamma^* \\ \delta\dot\varphi^*\end{bmatrix} = \begin{bmatrix} 0 & -\sin(\gamma^c)\omega_{nbx}^b + \cos(\gamma^c)\omega_{nbz}^b & 0 \\ \sec^2(\theta^c)\left(\sin(\gamma^c)\omega_{nbx}^b - \cos(\gamma^c)\omega_{nbz}^b\right) & \tan(\theta^c)\cos(\gamma^c)\omega_{nbx}^b + \tan(\theta^c)\sin(\gamma^c)\omega_{nbz}^b & 0 \\ \sec^2(\theta^c)\sin(\theta^c)\left(-\sin(\gamma^c)\omega_{nbx}^b + \cos(\gamma^c)\omega_{nbz}^b\right) & -\sec(\theta^c)\left(\cos(\gamma^c)\omega_{nbx}^b + \sin(\gamma^c)\omega_{nbz}^b\right) & 0 \end{bmatrix}\begin{bmatrix}\delta\theta \\ \delta\gamma \\ \delta\varphi\end{bmatrix} \quad (41)$$

According to Equation (41), the convected Euler angle errors can be written as:

$$\begin{bmatrix}\delta\theta^* \\ \delta\gamma^* \\ \delta\varphi^*\end{bmatrix} = \begin{bmatrix}\delta\theta_0 + \int_{t0}^t \delta\dot\theta^* dt \\ \delta\gamma_0 + \int_{t0}^t \delta\dot\gamma^* dt \\ \delta\varphi_0 + \int_{t0}^t \delta\dot\varphi^* dt\end{bmatrix} \quad (42)$$

From Equations (41) and (42), some conclusions can be obtained. Firstly, the convected Euler angle errors of SINS are affected by ω_{nbx}^b and ω_{nbz}^b, the angular velocity of the body frame with respect to the navigation frame is denoted in the body frame along the X and Z axes, not ω_{nby}^b along the Y axis. Secondly, the convected Euler angle errors are affected by the initial pitch error $\delta\theta_0$ and roll error $\delta\gamma_0$, rather than the initial head error $\delta\varphi_0$. Finally, the pitch magnitude greatly affects the propagation rules of convected Euler angle errors in the head and roll, but not pitch.

Since the state is an error vector, Equation (43) is an approximate expression which ignores the term as small as second order. According to Equations (29) and (41), the differential equation of the general Euler angle errors, including relative Euler angle errors and convected Euler angle errors, can be modeled as:

$$\begin{bmatrix}\delta\dot\theta \\ \delta\dot\gamma \\ \delta\dot\varphi\end{bmatrix} = \begin{bmatrix}\delta\dot\theta^* \\ \delta\dot\gamma^* \\ \delta\dot\varphi^*\end{bmatrix} + \begin{bmatrix}\delta\dot\theta^\otimes \\ \delta\dot\gamma^\otimes \\ \delta\dot\varphi^\otimes\end{bmatrix}$$

$$= \begin{bmatrix} 0 & -\sin(\gamma^c)\omega_{nbx}^b + \cos(\gamma^c)\omega_{nbz}^b & 0 \\ \sec^2(\theta^c)\left(\sin(\gamma^c)\omega_{nbx}^b - \cos(\gamma^c)\omega_{nbz}^b\right) & \tan(\theta^c)\cos(\gamma^c)\omega_{nbx}^b + \tan(\theta^c)\sin(\gamma^c)\omega_{nbz}^b & 0 \\ \sec^2(\theta^c)\sin(\theta^c)\left(-\sin(\gamma^c)\omega_{nbx}^b + \cos(\gamma^c)\omega_{nbz}^b\right) & -\sec(\theta^c)\left(\cos(\gamma^c)\omega_{nbx}^b + \sin(\gamma^c)\omega_{nbz}^b\right) & 0 \end{bmatrix}\begin{bmatrix}\delta\theta \\ \delta\gamma \\ \delta\varphi\end{bmatrix} +$$

$$\frac{1}{\cos(\theta^c)}\begin{bmatrix}\cos(\theta^c)\cos(\gamma^c) & 0 & \cos(\theta^c)\sin(\gamma^c) \\ \sin(\theta^c)\sin(\gamma^c) & \cos(\theta^c) & -\sin(\theta^c)\cos(\gamma^c) \\ -\sin(\gamma^c) & 0 & \cos(\gamma^c)\end{bmatrix} \quad (43)$$

$$\left\{\begin{bmatrix}\delta\omega_{ibx}^b + \varepsilon_x^b \\ \delta\omega_{iby}^b + \varepsilon_y^b \\ \delta\omega_{ibz}^b + \varepsilon_z^b\end{bmatrix} - \begin{bmatrix}c_{11} & c_{12} & c_{13} \\ c_{21} & c_{22} & c_{23} \\ c_{31} & c_{32} & c_{33}\end{bmatrix}\left\{\begin{bmatrix}0 & -\phi_V & \phi_N \\ \phi_V & 0 & -\phi_E \\ -\phi_N & \phi_E & 0\end{bmatrix}\begin{bmatrix}-\frac{V_N}{(R_M+H)} \\ \omega_{ie}\cos(L) + \frac{V_E}{(R_N+H)} \\ \omega_{ie}\sin(L) + \frac{V_E\tan(L)}{(R_N+H)}\end{bmatrix} + \begin{bmatrix}-\frac{\delta V_N}{(R_M+H)} + \frac{V_N\delta H}{(R_M+H)^2} \\ \frac{\delta V_E}{(R_N+H)} - \omega_{ie}\sin(L)\delta L - \frac{V_E\delta H}{(R_N+H)^2} \\ \frac{\tan(L)\delta V_E}{(R_N+H)} + \left(\omega_{ie}\cos(L) + \frac{V_E\sec^2(L)}{(R_N+H)}\right)\delta L - \frac{\tan(L)V_E\delta H}{(R_N+H)^2}\end{bmatrix}\right\}\right\}$$

According to Equation (43), the general Euler angle errors can be calculated by introducing the integral operation:

$$\begin{bmatrix}\delta\theta \\ \delta\gamma \\ \delta\varphi\end{bmatrix} = \begin{bmatrix}\delta\theta_0 + \int_{t0}^t \delta\dot\theta dt \\ \delta\gamma_0 + \int_{t0}^t \delta\dot\gamma dt \\ \delta\varphi_0 + \int_{t0}^t \delta\dot\varphi dt\end{bmatrix} \quad (44)$$

The singularity of the Euler angle error method can be avoided by different Euler angle rotation orders. Similarly, the differential equation of general Euler angle errors and conclusions can be obtained.

3. Simulation Experiments

The Euler angles are used for large-angle attitude movements, which are direct outputs of SINS. Compared with misalignment, the Euler angle error model is more important in some applications. The general Euler angle error model can be classified as the relative Euler angle error model or the convected Euler angle error model. In order to prove the validity of the proposed model, simulation experiments are carried out.

The simulation experiments are designed in large-angle attitude movements. Firstly, the proposed Euler angle error model can be established according to Equations (41)–(44). Then, the initial attitude, the initial Euler angle errors, and the rotational angular velocity can be set to describe large-angle attitude movements. Finally, the simulation experiments are carried out to verify the accuracy of the proposed model.

3.1. Simulation and Analysis of Convected Euler Angle Errors

In order to validate the proposed convected Euler angle error models (Equations (41) and (42)) and their conclusions, four simulation experiments are carried out, where the initial attitude of SINS is supposed by $\begin{bmatrix} \theta_0 & \gamma_0 & \varphi_0 \end{bmatrix} = \begin{bmatrix} -45° & -45° & -45° \end{bmatrix}$. In the first group simulation, there is the coupling of initial Euler angle errors in three axes $\begin{bmatrix} \delta\theta_0 & \delta\gamma_0 & \delta\varphi_0 \end{bmatrix} = \begin{bmatrix} 0.1° & 0.1° & 0.1° \end{bmatrix}$ and the rotation angular velocity of the body frame with respect to the navigation frame denoted in the body frame along the Y axis $\omega_{nby}^b = 1\,°/s$. The second group simulation presents the coupling of initial head errors $\delta\varphi_0 = 0.1°$, the rotation angular velocity of the body frame with respect to the navigation frame denoted in the body frame $\omega_{nb}^b = \begin{bmatrix} 1\,°/s & 1\,°/s & 1\,°/s \end{bmatrix}$. The coupling of initial Euler angle errors in three axes $\begin{bmatrix} \delta\theta_0 & \delta\gamma_0 & \delta\varphi_0 \end{bmatrix} = \begin{bmatrix} 0.1° & 0.1° & 0.1° \end{bmatrix}$ and the rotation angular velocity of the body frame with respect to the navigation frame denoted in the body frame along the X axis $\omega_{nbx}^b = 1\,°/s$ are given in the third group simulation. In the fourth group simulation, there is the coupling of initial Euler angle errors in three axes $\begin{bmatrix} \delta\theta_0 & \delta\gamma_0 & \delta\varphi_0 \end{bmatrix} = \begin{bmatrix} 0.1° & 0.1° & 0.1° \end{bmatrix}$ and the rotation angular velocity of the body frame with respect to the navigation frame denoted in the body frame, $\omega_{nb}^b = \begin{bmatrix} 1\,°/s & 1\,°/s & 1\,°/s \end{bmatrix}$.

The results of the four group simulation experiments are given in Figures 4–7, respectively. The convected Euler angle error model can precisely describe the attitude error propagation rules of SINS. When the SINS' attitude errors are regarded as error references, the root mean square error (RMSE) of the attitude angle error calculated by the convected Euler angle error model is superior to 0.4441″, as shown in Figures 4–7 and Table 1. The angular velocity in the Y axis ω_{nby}^b and the initial head error $\delta\varphi_0$ does not affect the convected Euler angle errors, which are greatly affected by the pitch magnitude. The conclusions above have been validated.
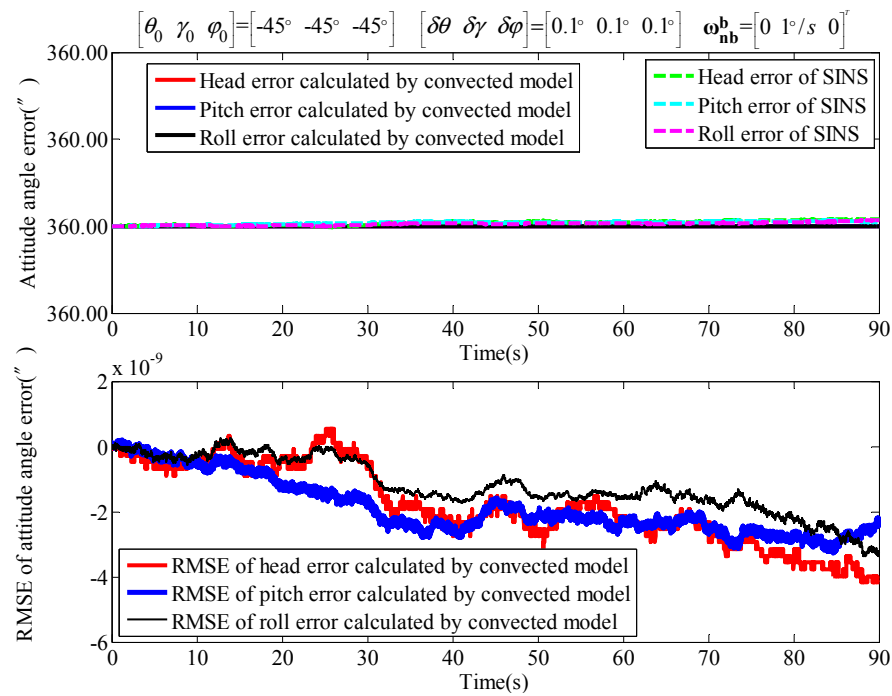
Figure 4. The first group I simulation with rotation in the Y axis ω_{nby}^{b}. RMSE: root mean square error.
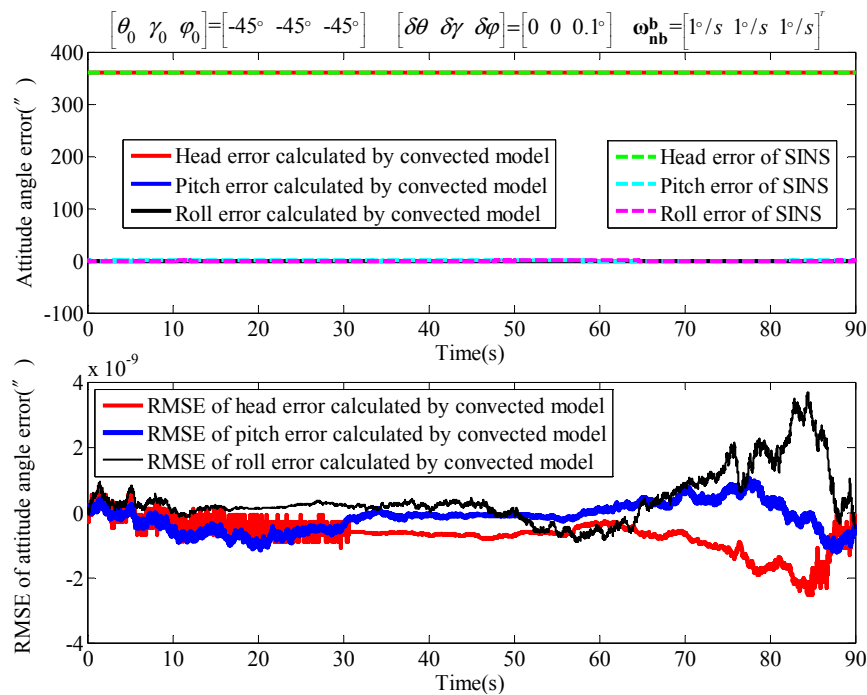

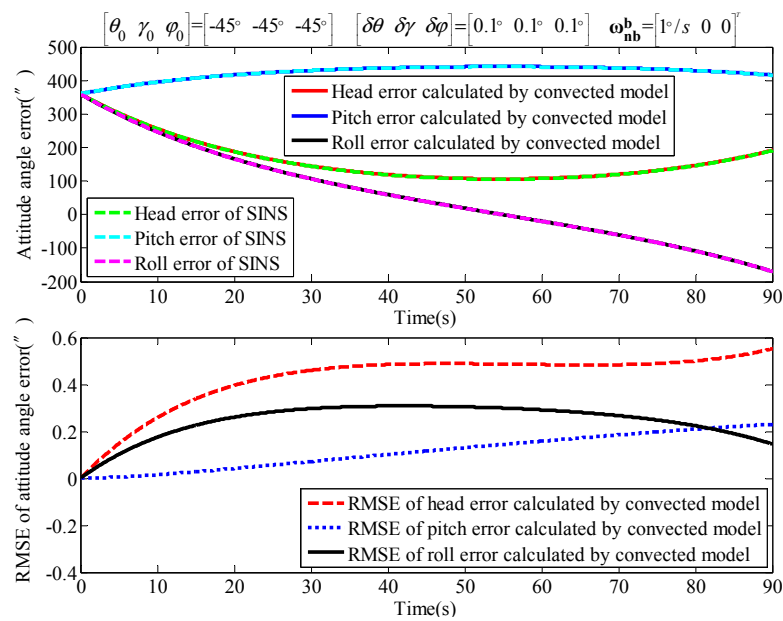**Figure 5.** The second group II simulation with the initial head error $\delta\varphi_0$.

Figure 6. The third group III simulation with rotation in the X axis ω^b_{nbx}.

Table 1. Attitude angle errors (RMSE (root mean square error)) solved by the convected Euler angle error model.

Simulations	Head Error $\delta\varphi^*$ ('')	Pitch Error $\delta\theta^*$ ('')	Roll Error $\delta\gamma^*$ ('')	Maximum Error ('')
First group I	2.168×10^{-9}	2.067×10^{-9}	1.471×10^{-9}	2.168×10^{-9}
Second group II	8.484×10^{-10}	4.571×10^{-10}	8.967×10^{-10}	8.967×10^{-10}
Third group III	0.4441	0.1350	0.2573	0.4441
Fourth group IV	0.2437	0.0405	0.2847	0.2847
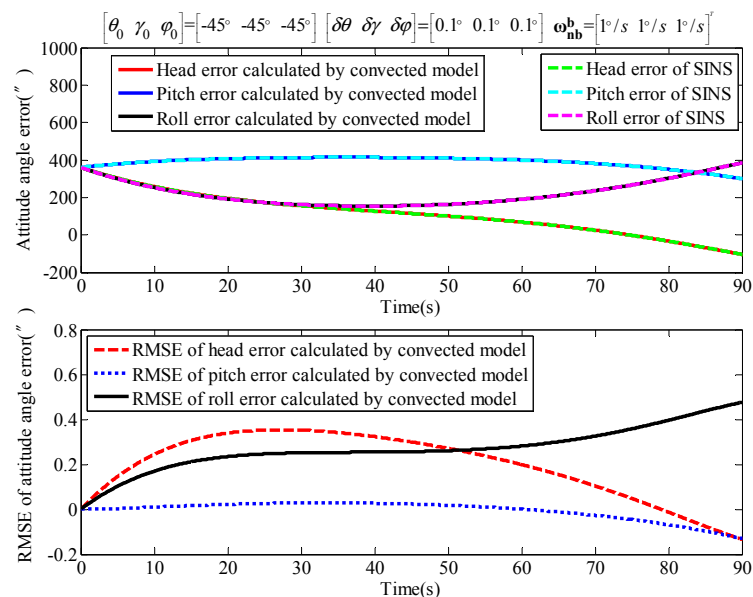
Figure 7. The fourth group IV simulation with coupling of the initial Euler angle errors and rotation in three axes.

3.2. Simulation and Analysis of General Euler Angle Errors

In order to validate the proposed general Euler angle error models (Equations (43) and (44)), three group simulation experiments are carried out, where the initial attitude and initial Euler angle errors of the SINS are respectively supposed as $\begin{bmatrix} \theta_0 & \gamma_0 & \varphi_0 \end{bmatrix} = \begin{bmatrix} -45° & -45° & -45° \end{bmatrix}$, $\begin{bmatrix} \delta\theta_0 & \delta\gamma_0 & \delta\varphi_0 \end{bmatrix} = \begin{bmatrix} 0.1° & 0.1° & 0.1° \end{bmatrix}$. In the three experiments, the SINS is driven to rotate with $1°/s$ in turn along the X, Y, and Z axes.

The results of three group simulation experiments are given in Figures 8–10. The general Euler angle error model can precisely describe the attitude error propagation rules of the SINS. When the SINS' attitude error is regarded as the reference, the RMSE of attitude angle errors calculated by the general Euler angle error model is shown in Figures 8–10 and Table 2. The RMSE of the proposed Euler angle error model is superior to 0.3195″, which is accurate enough. The simulation results prove the validity of the general Euler angle error model proposed.

The general Euler angle error model can accurately describe attitude error propagation rules, and it can be applied in the attitude movements. The proposed Euler angle error model can direct the response attitude movement status, especially in large-angle attitude movements. The attitude movement optimization can also be analyzed.

Table 2. Attitude angle errors (RMSE) calculated by the general Euler angle error model.

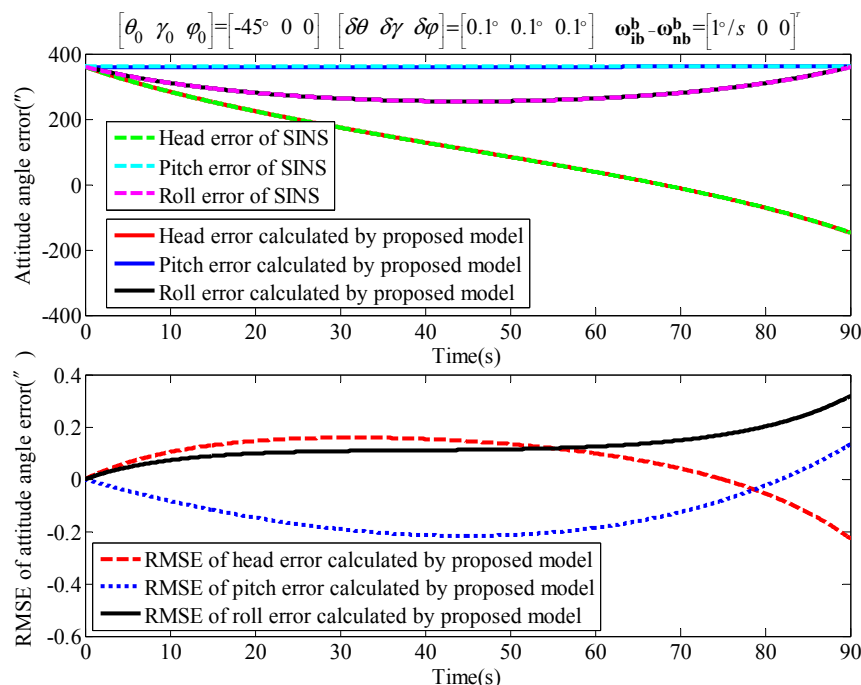| Simulations	Head Error $\delta\varphi^*$ (″)	Pitch Error $\delta\theta^*$ (″)	Roll Error $\delta\gamma^*$ (″)	Maximum Error (″)
First group I	0.1204	0.1536	0.1381	0.1536
Second group II	0.0018	0.0002	0.0015	0.0018
Third group III	0.1349	0.3195	0.1176	0.3195

Figure 8. The Euler angle error propagation with coupling of three initial Euler angle errors and rotation in the X axis.
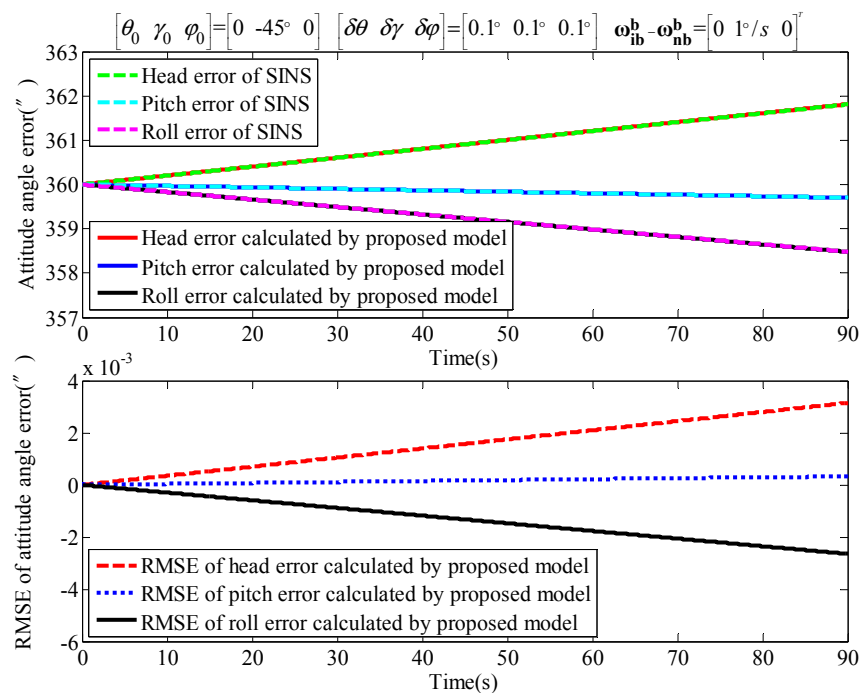
Figure 9. The Euler angle error propagation with coupling of three initial Euler angle errors and rotation in the *Y* axis.
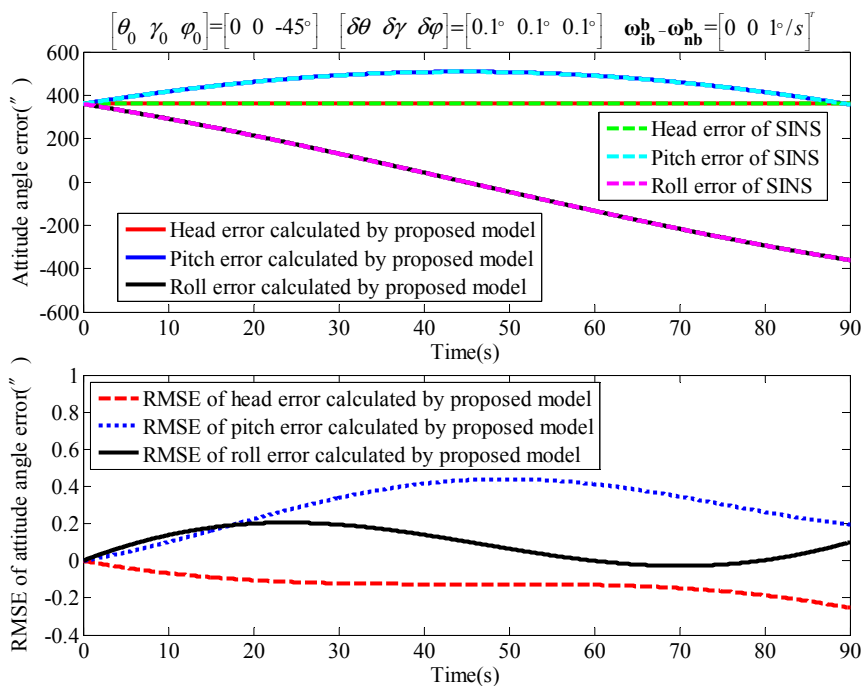

Figure 10. The Euler angle error propagation with the coupling of three initial Euler angle errors and rotation in the *Z* axis.

4. Discussion

There are some limitations of the proposed method. These above-mentioned experiments raised the idea that the proposed method can achieve sufficient accuracy for SINS. However, it does not perform well when there are three singularities. Therefore, the singularity problem of the Euler angle error method cannot be avoided by different Euler angle rotation orders. In practice, it is rare that the

Euler angles φ, θ, and γ, in turn along with head, pitch, and roll axes, have singularities at 90 degrees at the same time. Meanwhile, Euler angles are the direct output of the attitude change, and Euler angle errors can more accurately and rapidly characterize the attitude error propagation. The computational burden of the proposed method is reduced by avoiding attitude transformation compared with the conventional misalignment method. Consequently, the proposed method is applicable in most cases. Future work will address its application in a nonlinear environment.

5. Conclusions

The existing misalignment angle error model cannot directly describe the attitude error propagation, especially in large-angle attitude movements. The misalignment angle is a small angle, which is characterized by the calculation of the three-axis deviation angle between the computational frame and the navigation frame. Compared with the proposed general Euler angle error model, it does not reflect and optimize the body's attitude movement directly. Euler angles are the most intuitive measurements of attitude movements. The Euler angle errors of SINS, different from the misalignment of platform inertial navigation systems, comprise two parts: relative Euler angle errors and convected Euler angle errors. The proposed convected Euler angle error model and the general Euler angle error model, as well as their conclusions, have been validated by the simulation experiments. The general Euler angle error model can accurately describe attitude error propagation rules, which contribute to the design and operation of SINS. The attitude can be measured in real-time, then attitude movements can be optimized in large-angle attitude movements.

Author Contributions: Jianli Li and Pengfei Dang devised the algorithm and wrote the manuscript; and Yiqi Li and Bin Gu contributed to the design of the experiments and the discussion of the method. All the authors contributed in the English corrections and approved the final manuscript.

Conflicts of Interest: The authors declare no conflicts of interest.

Nomenclature

Notation

H	Height, m
L	Latitude, degree
ω	Angular velocity vector, rad/s
Φ	Misalignment, degree
$\delta\omega_{inx}^{b}$	The angular velocity error of the navigation frame with respect to the inertial Frame denoted in the body frame along X axis, rad/s
$\delta\omega_{iny}^{b}$	The angular velocity error of the navigation frame with respect to the inertial Frame denoted in the body frame along Y axis, rad/s
$\delta\omega_{inz}^{b}$	The angular velocity error of the navigation frame with respect to the inertial Frame denoted in the body frame along Z axis, rad/s
$\begin{bmatrix} \delta\theta^{\otimes} & \delta\gamma^{\otimes} & \delta\varphi^{\otimes} \end{bmatrix}^{T}$	The relative Euler angle error, rad
$\begin{bmatrix} \delta\dot{\theta}^{*} & \delta\dot{\gamma}^{*} & \delta\dot{\varphi}^{*} \end{bmatrix}^{T}$	The convected Euler angle error, rad

Subscripts

i	The inertial frame
b	The body frame
n	The navigation frame
e	The Earth frame
c	The computational frame

References

1. Wang, J.H.; Gao, Y. Land vehicle dynamics-aided inertial navigation. *IEEE Trans. Aerosp. Electron. Syst.* **2010**, *46*, 1638–1653. [CrossRef]
2. Wu, Y.X.; Hu, X.P.; Wu, M.P. Strapdown inertial navigation, using dual quaternion algebra: Error analysis. *IEEE Trans. Aerosp. Electron. Syst.* **2006**, *42*, 259–266.
3. Cao, Q.; Zhong, M.Y.; Guo, J. Non-linear estimation of the flexural lever arm for transfer alignment of airborne distributed position and orientation system. *IET Radar Sonar Navig.* **2015**, *11*, 41–51. [CrossRef]
4. Li, J.L.; Fang, J.C.; Du, M. Error analysis and gyro biases calibration of analytic coarse alignment for airborne POS. *IEEE Trans. Instrum. Meas.* **2012**, *61*, 3058–3064.
5. Liu, X.X.; Zhao, Y.; Liu, Z.P.; Wang, L.H. A novel self-alignment method for SINS based on parameter recognition and dual-velocity vectors. *Proc. Inst. Mech. Eng. Part G J. Aerosp. Eng.* **2015**, *229*, 2151–2162. [CrossRef]
6. Wu, Y.X.; Pan, X.F. Velocity/position integration formula part I: Application to in-flight coarse alignment. *IEEE Trans. Aerosp. Electron. Syst.* **2013**, *49*, 1006–1023. [CrossRef]
7. Wu, Y.X. Further results on "velocity/position integration formula (I): Application to in-flight coarse alignment". *IEEE Trans. Aerosp. Electron. Syst.* **2015**, *51*, 773–775. [CrossRef]
8. Goshen, M.D.; Bar, I.I.Y. Unified approach to inertial navigation system error modeling. *J. Guid. Control Dyn.* **1992**, *15*, 648–653. [CrossRef]
9. Fang, J.C.; Gong, X.L. Predictive iterated Kalman filter for INS/GPS integration and its application to SAR motion compensation. *IEEE Trans. Instrum. Meas.* **2010**, *59*, 909–915. [CrossRef]
10. Arshal, G. Error equations of inertial navigation. *J. Guid. Control Dyn.* **1987**, *10*, 351–358. [CrossRef]
11. Silva, F.O.; Hemerly, E.M.; Filho, W.C.L. Error Analysis of Analytical Coarse Alignment Formulations for Stationary SINS. *IEEE Trans. Aerosp. Electron. Syst.* **2016**, *52*, 1777–1796. [CrossRef]
12. Hao, Y.L.; Gong, J.; Gao, W.; Li, L. Research on the dynamic error of strapdown inertial navigation system. In Proceedings of the IEEE International Conference on Mechatronics and Automation, Takamatsu, Japan, 5–8 August 2008; pp. 814–819.
13. Xiong, J.; Guo, H.; Yang, Z.H. A two-position SINS initial alignment method based on gyro information. *Adv. Space Res.* **2014**, *53*, 1657–1663. [CrossRef]
14. Chang, G.B. Fast two-position initial alignment for SINS using velocity plus angular rate measurements. *Adv. Space Res.* **2015**, *56*, 1331–1342. [CrossRef]
15. Chen, K.; Zhao, G.; Meng, Z. Equivalent approaches to equations of traditional transfer alignment and rapid transfer alignment. In Proceedings of the 7th World Congress on Intelligent Control and Automation, Chongqing, China, 25–27 June 2008; pp. 892–895.
16. Wang, M.S.; Wu, W.Q.; Wang, J.L.; Pan, X.F. High-order attitude compensation in coning and rotation coexisting environment. *IEEE Trans. Aerosp. Electron. Syst.* **2015**, *51*, 1178–1190. [CrossRef]
17. Savage, P.G. Analytical modeling of sensor quantization in strapdown inertial navigation error equations. *J. Guid. Control Dyn.* **2002**, *25*, 833–842. [CrossRef]
18. Zhong, M.Y.; Gao, S.S.; Li, W. A quaternion-based method for SINS/SAR integrated navigation system. *IEEE Trans. Aerosp. Electron. Syst.* **2012**, *48*, 514–524. [CrossRef]
19. Lu, J.J.; Xie, L.L.; Li, B.G. Applied quaternion optimization method in transfer alignment for airborne AHRS under large misalignment angle. *IEEE Trans. Instrum. Meas.* **2016**, *65*, 346–354. [CrossRef]
20. Jing, W.X.; Xia, X.W.; Gao, C.S.; Wei, W.S. Attitude control for spacecraft with swinging large-scale payload. *Chin. J. Aeronaut.* **2011**, *24*, 309–317. [CrossRef]
21. Janota, A.; Šimák, V.; Nemec, D. Improving the precision and speed of Euler angles computation from low-cost rotation sensor data. *Sensors* **2015**, *15*, 7016–7039. [CrossRef] [PubMed]
22. Zheng, L.L.; Jiang, Y.X. A single CCD algorithm to determine the position and attitude during rolling phase of rendezvous and docking. *Digit. Manuf. Autom.* **2012**, *190–191*, 813–818. [CrossRef]
23. Taki, S.; Nenchev, D. Euler angle based feedback control of large eigenaxis rotations in the presence of singularities and model uncertainty. In Proceedings of the International Conference on Control, Automation and Systems, Gwangju, Korea, 20–23 October 2013; pp. 34–39.

24. Wu, Z.W.; Yao, M.L.; Ma, H.G.; Jia, W.M.; Tian, F.H. Low-cost antenna attitude estimation by fusing inertial sensing and two-antenna GPS for vehicle-mounted satcom-on-the-move. *IEEE Trans. Veh. Technol.* **2013**, *62*, 1084–1096. [CrossRef]

25. Bozek, P.; Al Akkad, M.A.; Blištan, P.; Ibrahim, N.I. Navigation control and stability investigation of a mobile robot based on a hexacopter equipped with an integrated manipulator. *Int. J. Adv. Robot. Syst.* **2017**, *14*, 1–13. [CrossRef]

26. Hunt, J.; Lee, H.; Artemiadis, P. A novel shoulder exoskeleton robot using parallel actuation and a passive slip interface. *J. Mech. Robot. Trans. ASME* **2017**, *9*, 1–7. [CrossRef]

27. Klein, J.; Spencer, S.J.; Reinkensmeyer, D.J. Breaking it down is better: Haptic decomposition of complex movements aids in robot-assisted motor Learning. *IEEE Trans. Neural Syst. Rehabil. Eng.* **2012**, *20*, 268–275. [CrossRef] [PubMed]

28. Toz, M.; Kucuk, S. Dynamics simulation toolbox for industrial robot manipulators. *Comput. Appl. Eng. Educ.* **2010**, *18*, 319–330. [CrossRef]

29. Ruzaij, M.F.; Neubert, S.; Stoll, N.; Thurow, K. Multi-sensor robotic-wheelchair controller for handicap and quadriplegia patients using embedded technologies. In Proceedings of the International Conference on Human System Interactions, Portsmouth, UK, 6–8 July 2016; pp. 103–109.

30. Phillips, W.F.; Hailey, C.E.; Gebert, G.A. Review of attitude representations used for aircraft kinematics. *J. Aircr.* **2001**, *38*, 718–737. [CrossRef]

31. Lee, J.H.; Shin, S.S.; Yoon, S.J. A comparison study of real-time solution to all-attitude angles of an aircraft. *J. Mech. Sci. Technol.* **2006**, *20*, 376–381.

32. Xia, X.W.; Jing, W.X.; Li, C.Y.; Gao, C.S. Time-shared scheme design for attitude control system during space separation. *Aerosp. Sci. Technol.* **2011**, *15*, 108–116. [CrossRef]

33. Hu, P.D.; Wang, S.Y.; Zhang, R.; Liu, X.X.; Xu, B. Fast heading-rotation-based high-accuracy misalignment angle estimation method for INS and GNSS. *Measurement* **2017**, *102*, 208–213. [CrossRef]